

On–Off–On Fluorescent Carbon Dot Nanosensor for Recognition of Chromium(VI) and Ascorbic Acid Based on the Inner Filter Effect

Min Zheng,[†] Zhigang Xie,^{*,‡} Dan Qu,^{†,§} Di Li,[†] Peng Du,^{†,§} Xiabin Jing,[‡] and Zaicheng Sun^{*,†}

[†]State Key Laboratory of Luminescence and Applications, Changchun Institute of Optics, Fine Mechanics, and Physics, Chinese Academy of Sciences, 3888 East Nanhu Road, Changchun, Jilin 130033, P. R. China

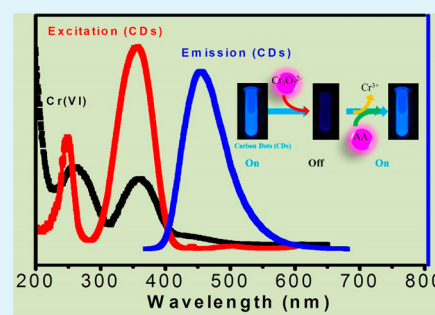
[‡]State Key Laboratory of Polymer Physics and Chemistry, Changchun Institute of Applied Chemistry, Chinese Academy of Sciences, 5625 Renmin Street, Changchun, Jilin 130022, P. R. China

[§]University of Chinese Academy of Sciences, Beijing 100049, P. R. China

Supporting Information

ABSTRACT: Chromium(VI) [Cr(VI)] is considered as a severe environmental pollutant, due to its highly toxic and carcinogenic properties. Therefore, low cost, highly sensitive sensors for the determination of Cr(VI) are highly demanded. It is well-known that highly luminescent carbon dots (CDs) have been successfully applied as fluorescent nanosensors for pH, ions, and molecular substances. In the present work, we have demonstrated an on–off fluorescent CD probe for detecting Cr(VI) based on the inner filter effect (IFE) because the absorption bands of Cr(IV) fully covered the emission and excitation bands of CDs. This CD-based nanosensor provides obvious advantages of simplicity, convenience, rapid response, high selectivity, and sensitivity, which have potential application for the detection of Cr(VI) in the environmental industry. In addition, because Cr(VI) can be reduced to low valent chromium species easily by reductant, resulting in the elimination of the IFE and recovery of CD fluorescence, the CD–Cr(VI) mixture could behave as an off–on type fluorescent probe for reductant. We employed ascorbic acid (AA) as an example molecule to demonstrate this off–on type fluorescent probe.

KEYWORDS: on–off–on fluorescent, carbon dots, nanochemosensor, inner filter effect (IFE), chromium(VI), ascorbic acid



INTRODUCTION

During the last decades, industrial and other anthropogenic processes have been constantly releasing heavy-metal ions into the environment, among which chromium(VI) [Cr(VI)]^{1,2} is more hazardous to public health compared to other valence states, such as Cr(0) and Cr(III), because of its greater mobility and carcinogenic properties. Therefore, the determination of Cr(VI) in environmental samples is of great importance, and the concentration of Cr(VI) in drinking water is strictly regulated to a lower micromolar level by many nations.³ To monitor the quality of drinking water and lower the risks of industrial wastes, high sensitivity and fast response analytical methods are greatly required to ensure the Cr(VI) determination at low concentration levels. Moreover, good selectivity is also necessary to tolerate the interference of some coexisting foreign ions,⁴ such as Na⁺, K⁺, Ca²⁺, Mg²⁺, Al³⁺, Fe³⁺, Co²⁺, Ni²⁺, Cu²⁺, Zn²⁺, Hg²⁺, Cl⁻, SO₄²⁻, and NO₃⁻. In the past 20 years, numerous analytical techniques for the determination of Cr(VI) in different sample matrices have been successfully developed, including chromatography,⁵ spectrofluorimetry,⁶ and atomic absorption spectrometry,⁷ etc. However, most of these methods are not so convenient due to the requirement of expensive equipment and complicated sample pretreatment. Therefore, a simple, sensitive, and selective method for Cr(VI) detection is highly demanded. With the distinct advantages of

high sensitivity, selectivity, and easy operation, the fluorescence-based probe for the detection of Cr(VI) is a good alternative. Up to date, the reported chemosensors for Cr(VI) are relatively few.^{6,8} Furthermore, CD-based fluorescent nanochemosensors for Cr(VI) have never been studied. On the other hand, ascorbic acid (AA), also known as vitamin C, is an antioxidant that is a vital vitamin in the diet of humans and has been used for the prevention and treatment of the common cold, mental illness, cancer, and AIDS.⁹ Therefore, the analysis of AA content in food products and pharmaceutical preparations has received considerable attention, and it is essential to develop a simple and rapid method for its determination in routine analysis. Although various methods have been employed for the quantitative determination of AA,¹⁰ efforts continue the search for even better methods to determine the amount of AA.

Compared with classic quantum dots and fluorescent molecules, carbon dots (CDs) possess a series of merits such as low cost, simple synthesis route, better biocompatibility, lower cytotoxicity, high photo and chemical stability, no blinking fluorescence, and tunable excitation and emission

Received: September 27, 2013

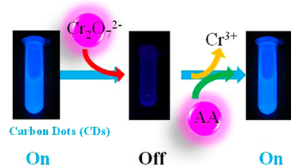
Accepted: November 25, 2013

Published: November 25, 2013

spectra.^{11–16} These properties enable development of CD-based fluorescent nanosensors for the detection of pH,^{17–19} ions (such as Hg²⁺, Cu²⁺, Ag⁺, Fe³⁺, and PO₄³⁻, etc.),^{20–26} and molecular substances (for instance, DNA, nitrite, glucose, and biothiol etc.)^{27–30} by monitoring the changes of their fluorescence intensity. On the basis of different photophysical processes, conventional sensing mechanisms including photo-induced electron transfer (PET), intramolecular charge transfer (ICT), twisted intramolecular charge transfer (TICT), metal–ligand charge transfer (MLCT), electronic energy transfer (EET), and fluorescence resonance energy transfer (FRET) are employed for the fluorescent chemosensor.³¹ In general, the sensing process based on the above mechanisms involves the intermolecular interaction between the chemosensor and target molecule. It only works when they are at a particular distance or have a complementary geometry, leading to the method being complicated and time-consuming and therefore to restricted practical applications. An alternative way to design fluorescent assays is based on the inner filter effect (IFE), which is known to result from the absorption of the exciting and/or emitted light by absorbers in the detection system,^{32–37} and an enhanced sensitivity for this method could be obtained compared to other mechanisms because the changes in the absorbance of sensors transform exponentially into fluorescence intensity changes. However, a rare CD-based nanosensor via fluorescent inner filter effect (IFE) was never developed.

In this paper, we first developed a facile thermal pyrolysis route to prepare CDs with high quantum yield (QY, 88.6%) using citric acid (CA) as the carbon source and diethylenetriamine (DETA) as the surface passivation agent. CDs were used as IFE-based fluorescent chemosensors for the determination of Cr(VI) by a significant fluorescence quenching (on–off, Scheme 1), and they have lots of advantages over other

Scheme 1. Schematic Illustration of Fluorescence Assays for Cr(VI) and AA Based on the Inner Filter Effect (IFE) of CDs



reported methods: mild condition (room temperature in weak acid solution), faster response (within 1 min), higher sensitivity ($K_{SV} = 6.90 \times 10^4$ L/mol). Moreover, the CD–Cr(VI) mixture could behave as a “turn-on” fluorescent sensor (off–on, Scheme 1) for detection of AA with fast response (within 1 min) and high sensitivity. To the best of our knowledge, this is the first demonstration of a fluorescent nanosensor for Cr(VI) and AA based on the IFE.

EXPERIMENTAL SECTION

Materials. All reagents were purchased from commercial sources and used without further treatment.

Deionized water (distilled) was used throughout the experiment as the solvent. All the reagents were purchased from commercial suppliers (Beijing Chemical Reagent Co., China; Acros; Fluka) and used without further purification. The solution of Cr(VI) was prepared from K₂Cr₂O₇. The solutions of metal ions were prepared from their nitrate, sulfate, or chloride salts.

Cr(VI) stock solution (1.00×10^{-3} mol/L) was prepared as follows: 14.7 mg of potassium dichromate (K₂Cr₂O₇) was dissolved in 5 mL of water and then diluted to 100 mL in a standard flask.

Cr(VI) stock solutions of 1.00×10^{-4} and 1.00×10^{-5} mol/L were prepared by diluting the original stock solution, and the proper amount of these solutions was used in the analytical procedure.

Synthesis of Carbon Dots (CDs). Typically, 2.10 g (10 mmol) of CA was added into 3.5 g (~35 mmol) of diethylenetriamine (DETA). The reaction was heated from room temperature to 170 °C in an oil bath and held at 170 °C for 30 min. Then the reaction flask was taken out of the oil bath and naturally cooled to room temperature. Then acetone was added into the reaction, and the precipitation was collected by centrifugation. Then white solid was placed in a dialysis bag (cutoff M_n : 3.0 kDa) and dialyzed against water for 2 days to remove small molecules. The water was replaced every 6 h, and finally, CDs in the dialysis bag were freeze-dried to a yellow solid.

Characterization. High-resolution transmission electron microscopy (HRTEM) images and fast Fourier transform (FFT) spot diagrams were recorded with an FEI-TECNAI G² transmission electron microscope operating at 200 kV. Fourier transform infrared (FT-IR) spectra of CDs were recorded as KBr pellets with a Bruker Vertex 70 spectrometer from 4000 to 500 cm⁻¹. Fluorescence emission spectra were recorded on an LS-55 fluorophotometer. UV–vis absorption spectra were conducted on a Shimadzu UV-2450 spectrophotometer. The crystalline structure was recorded by using an X-ray diffractometer (XRD) (Bruker AXS D8 Focus), using Cu K α radiation ($\lambda = 1.54056$ Å). X-ray photoelectron spectra were obtained on a Thermo Scientific ESCALAB 250 Multitechnique Surface Analysis.

Quantum Yield Determination. The relative quantum yields of the CDs were measured in reference to Cumarin 1 (QY 73.0% at 360 nm excitation). The same excitation wavelength, gain, and slit band widths are applied for the two samples, and the formula used for QY measurements is as follows

$$QY = QY_{\text{ref}} \frac{\eta^2 I A_{\text{ref}}}{\eta_{\text{ref}}^2 A I_{\text{ref}}}$$

where QY_{ref} is the quantum yield of the reference compound; η is the refractive index of the solvent; I is the integrated fluorescence intensity; and A is the absorbance at the excitation wavelength. To minimize reabsorption effects, absorbencies in the 10 mm fluorescence cuvette were kept under 0.1 at the excitation wavelength (360 nm).

General Procedure for Fluorescence Titration. Fluorescence titration of CDs with Cr(VI) was performed as follows: 2 mL of CD solution (0.5 $\mu\text{g}/\text{mL}$) was taken into the cuvette, and then certain equivalents of Cr(VI) were added stepwise to CD solution by a microinjector. As a very small amount of Cr(VI) was added, the final volume of the solution was nearly unchanged (2 mL). The mixed solution was incubated within 1 min and then excited at 360 nm. The corresponding emission values during titrations were recorded.

RESULTS AND DISCUSSION

In typical CDs preparation, CA does not dissolve in DETA at room temperature (RT). When the reaction mixture was heated in an oil bath from RT to 170 °C, the white solid CA turned into sticky solid at ~110 °C and then into light yellow gel at ~140 °C. The color of the gel turned into yellow and orange, and the gel became transparent liquid when the reaction temperature exceeded 150 °C due to the melting of CA at 153 °C. The reaction bottle was removed from the oil bath when the reaction temperature reached 170 °C for 30 min and then naturally cooled to RT. The reaction solution emitted very bright blue light (Figure S1, Supporting Information). Then acetone was added into the reaction mixture, and the white precipitate was collected by centrifugation. Finally, the solid was placed in a dialysis bag (cutoff M_n : 3.0 kDa) and dialyzed against water for 2 days to remove small molecules and

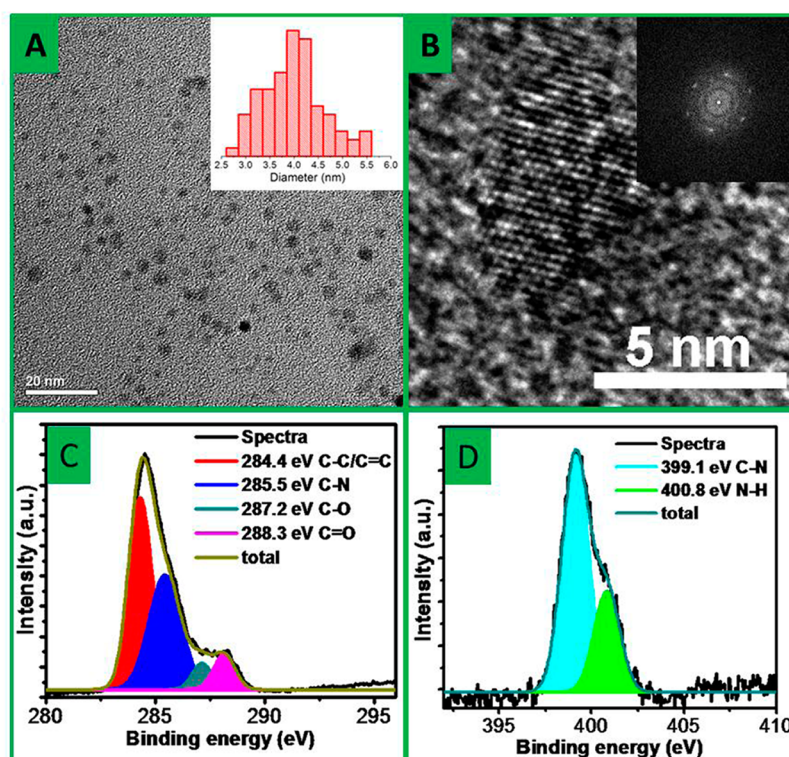


Figure 1. TEM (A) and high-resolution TEM (B) images of CDs. Insets are the corresponding particles size distribution and fast fourier transform image. High-resolution C 1s (C) and N 1s (D) XPS spectra of CDs.

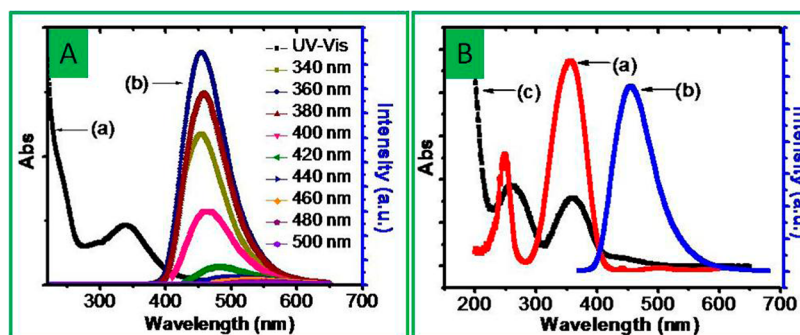


Figure 2. (A) UV-vis absorption (a) and photoluminescent spectra (b) of CDs under different excitation wavelengths. (B) fluorescence excitation (a) and emission (b) spectra of CDs and UV-vis absorption spectrum of Cr(VI) (c).

freeze-dried to obtain yellow CD product (Figure S2, Supporting Information).

The morphology and structure of CDs were confirmed by transmission electron microscopy (TEM). TEM images (Figure 1A) show that the size of the as-prepared CDs is distributed in the range from 3 to 5.5 nm, with an average size of 4.0 nm. By the high-resolution TEM (Figure 1B), most particles are observed to have a discernible lattice structure. Various lattice planes can be clearly identified with spacings of 0.21 and 0.245 nm, which correspond to the (103) diffraction plane of diamond-like (sp^3) carbon and the (100) facet of graphitic carbon, respectively. The fast Fourier transform micrograph in the inset of Figure 1B reveals characterized diffraction patterns of (103) and (100) facets of CDs.^{38,39} The XRD patterns of the CDs displayed three broad peaks centered at 5.3, 3.4, and 2.14 Å, which are attributed to disordered carbon atoms, and the graphite lattice spacing (Figure S3, Supporting Information). The Raman spectra of the CDs (Figure S4, Supporting

Information) display two broad peaks at around 1451 and 1604 cm^{-1} , which are attributed to the D band (sp^3 -hybridized) and G band (sp^2 -hybridized), respectively, indicating that they have a structure similar to graphite. FT-IR spectra (Figure S5, Supporting Information) were used to identify the surface functional groups present on carbon dots. The broad absorption bands at 3000–3500 cm^{-1} are assigned to stretching vibrations of O–H and N–H, and the bands at 1636 and 1210 cm^{-1} are attributed to the vibrational absorption band of C=O and Ph–O groups, respectively. The bands at 1569 and 1311 cm^{-1} are from the bending vibrations of N–H and C–NH, respectively. That indicates that there are lots of amino groups on the surface of CDs. The peaks at 1050 and 1090 cm^{-1} related to the C–OH stretching vibrations imply the existence of large numbers of hydroxyl groups. These functional groups improve the hydrophilicity and stability of the CDs in an aqueous system, which is conducive to the applications of CDs in the area of fluorescence probes. The X-ray photoelectron

spectroscopy (XPS) spectra (Figure S6, Supporting Information, and Figure 1C and 1D) of the CDs exhibit three peaks at 285.0, 398.8, and 530.6 eV, which are attributed to C 1s, N 1s, and O 1s, respectively. The high-resolution XPS spectra of C 1s (Figure 1C) can be well deconvoluted into four surface components, corresponding to sp^2 (C=C/C-C) at binding energy of 284.4 eV, C-N at 285.5 eV, C-O at 287.2 eV, and C=O at 288.3 eV. The high-resolution XPS spectrum of N 1s (Figure 1D) exhibits two peaks at 399.1 and 400.8 eV, related to pyridinic and pyrrolic N, respectively. That indicates that N was doped into the graphite structure in the CDs. The surface components of the CDs determined by the XPS are in good agreement with FT-IR results.

Figure 2A shows the UV-vis absorption and photoluminescent spectra of CDs under different excitation wavelengths. As shown in Figure 2A(a), CDs have two absorption bands: one located at 240 nm likely originates from the formation of multiple polyaromatic chromophores, and the other one centered at 340 nm is ascribed to the $n-\pi^*$ transition of CDs. The results of photoluminescent spectra of CDs [Figure 2A(b)] indicate that the emission wavelength of CDs is nearly excitation-independent when the excitation wavelength is less than 400 nm with the maximum excitation wavelength and the maximum emission wavelength at 360 and 456 nm, respectively. Moreover, the PL lifetime also shows excitation-independent and remains constant under excitation of 300–400 nm, and the PL decay of the CDs was deconvoluted using a monoexponential decay function to yield a lifetime of 13.0 ns (Figure S7, Supporting Information). The results of PL spectra and decay of CDs further confirmed that both the size and the surface state of CDs are uniform.^{40–42} The relative PL QY of CDs is as high as 88.6% in reference to coumarin 1 (73.0% at 360 nm excitation), which is helpful for acting as a highly sensitive chemosensor. The stability of the as-prepared CDs is examined by long-time monitoring of fluorescent emission, which shows negligible change of fluorescent intensity at ~ 456 nm under visible light for 18 h (Figure S8, Supporting Information).

A high efficiency of the IFE needs a good spectral overlap between the absorption band of the absorber and the excitation band and/or emission band of the fluorophore. Therefore, it is important to choose a suitable absorber and fluorophore pair for the IFE-based fluorescent chemosensor. As shown in Figure 2B, the excitation spectrum of CDs has two bands at 250 and 358 nm (a), and the emission band of CDs under the excitation of 360 nm is centered at 456 nm (b); however, Cr(VI) exhibits broad absorption at 260, 360, and 440 nm (c), respectively, showing quite precise overlapping with the excitation and emission bands of CDs. As a consequence, Cr(VI) can not only shield the excitation light for CDs but also absorb the emission light from CDs. Therefore, the absorbance enhancement of Cr(VI) could be successfully converted to fluorescence quenching of CDs, which ensures that the IFE occurs in a highly efficient way.

To achieve sensitive detection of Cr(VI), the effect of pH value in analyte solution on the fluorescence of CDs was investigated. The response was independently tested three times at each pH, and an average value was calculated. As shown in Figure 3 and Figure S9 (Supporting Information), the fluorescence intensity of CDs changes slightly within a broad pH range of 2–11.4, indicating that this pH range has little effect on the fluorescence intensity of the CDs. Herein, the pH values of our stock solutions of Cr(VI) are in the pH range of

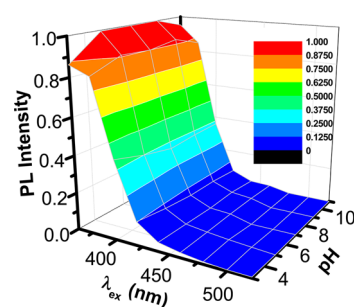


Figure 3. Photoluminescent spectra of CDs under the excitation of 360 nm at different pH solution.

5–6, in which $HCrO_4^-$ and CrO_4^{2-} coexist.⁴³ Thus, the fluorescence intensity of CDs ($0.5 \mu\text{g/mL}$) was monitored at a solution pH value of ~ 6 . Furthermore, to optimize the analytical procedure, the effect of incubation time and CD concentration were investigated. The kinetic characteristics of the reaction system were investigated and shown in Figure S10 (Supporting Information). Upon the addition of 0.05 mmol/L of Cr(VI) to $0.5 \mu\text{g/mL}$ of CDs solution, a stable fluorescent signal at 456 nm could be obtained within a reaction time of 1 min. CDs possess high resistance to photobleaching, and the fluorescence intensity remains constant for at least 2 h. Therefore, a 1 min incubation time is enough for the fluorescence quenching measurement. The results in Figure S11 (Supporting Information) indicate that when $0.25\text{--}10 \mu\text{g/mL}$ of CDs are mixed with 0.05 mmol/L of Cr(VI) for 1 min a maximum fluorescence quenching is observed for $0.5 \mu\text{g/mL}$ of CD solution. Thus, in this work, $0.5 \mu\text{g/mL}$ of CDs is applied to the determination of Cr(VI) at the lower micromolar level to ensure the acceptable reaction rate. To evaluate the selectivity of Cr(VI) detection, interferences of foreign ions toward CDs were studied under the optimum experimental conditions: $0.5 \mu\text{g/mL}$ of CDs, 1 min incubation time, excitation/emission at 360/456 nm at room temperature. As shown in Table 1 and

Table 1. Tolerance of Foreign Ions in the Determination of 1.0×10^{-4} mol/L of Cr(VI)

ions added	tolerance ratio (mol/mol)
NO_3^- , Cl^-	400
SO_4^{2-} , Na^+ , Mg^{2+} , Ca^{2+}	200
Al^{3+}	100
Fe^{2+} , Zn^{2+}	50
Cu^{2+}	10
Fe^{3+}	5
MnO_4^-	0.2

Figure S12 (Supporting Information), to ensure a relative error within 3.0% for Cr(VI) detection, most ions could be allowed to coexist at a concentration of >100-fold of Cr(VI). Fe^{2+} and Zn^{2+} have negligible interference when their concentration is no more than 50-fold of Cr(VI). Cu^{2+} and Fe^{3+} have mild interference and should be kept lower than 10- and 5-fold, respectively. The major interference is MnO_4^- which is a deep purple color and has absorption across a wide range of wavelengths from the UV to visible region; therefore, the tolerance ratio is 0.2. In summary, it is possible to use CDs as a fluorescent probe for Cr(VI) detection in chromium contamination of soil and groundwater.

According to the above procedure, sensitivity and linear response range of the CD-based sensing system are measured. As shown in Figure 4 and Figure S13 (Supporting

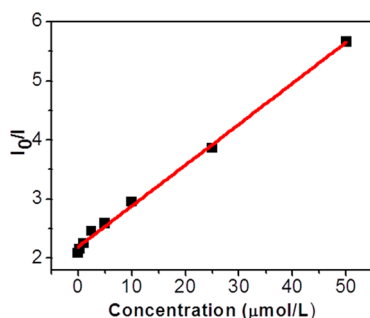


Figure 4. Stern–Volmer plot of CDs quenched by Cr(VI) aqueous solution.

Information), the linear range is 0.01–50 $\mu\text{mol/L}$ (i.e., 0.52–2600 $\mu\text{g/L}$) of Cr(VI), in which the fluorescence intensity vs the [Cr(VI)] plot can be curve-fitted into $(I_0/I) - 1 = K_{SV}[\text{Cr(VI)}] + 1.19$, close to the Stern–Volmer equation. The K_{SV} value is calculated to be 6.90×10^4 L/mol with a correlation coefficient R^2 of 0.998. According to the World Health Organization (WHO),³ Cr(VI) concentrations lower than 50 $\mu\text{g/L}$ are acceptable in drinking water, which means that our IFE-based fluorescent method was sensitive enough to monitor Cr(VI) concentration in drinking water. This CD-based “turn-off” fluorescent probe via IFE provides obvious advantages of simplicity, convenience, and rapid implementation and thus has potential application for the detection of Cr(VI) in the environmental industry.

Reduction reactions of Cr(VI) in the presence of AA have received a great deal of attention because of the important role that AA plays in removing Cr(VI) as a pollutant and because the reaction of Cr(VI) with AA can be carried out under very mild conditions (room temperature, in acidic or even weak alkaline solutions, etc.).^{44,45} For our CDs–Cr(VI) system, Cr(VI) could be smoothly reduced to Cr(III) by AA, resulting in the elimination of the IFE and recovery of CD fluorescence. Therefore, the CD–Cr(VI) system could behave as a “turn-on” fluorescent sensor for detection of AA. As shown in Figure 5A, the fluorescence of the CD–Cr(VI)/AA mixture was enhanced gradually with increasing concentration of AA. A good linear relationship of fluorescence intensity and AA concentration is observed from 0.03 to 0.1 mmol/L (Figure 5B), with a linear equation of $I = 1.22 \times 10^6 [\text{AA}] (\text{mol/L}) - 21.5$ ($R = 0.993$).

This CD–Cr(VI)-based “turn-on” fluorescent nanosensor provides obvious advantages of simplicity, convenience, and rapid implementation.

CONCLUSIONS

In summary, we have demonstrated the rationale of a simple, time-saving, and economical on–off–on fluorescent method for detection of Cr(VI) and AA using CDs as a fluorescent nanosensor based on the IFE. Compared with conventional fluorescent chemosensors, the present one appears to be more sensitive and selective and has potential application for the detection of Cr(VI) in the environmental industry and AA.

ASSOCIATED CONTENT

Supporting Information

Additional images, XRD, Raman, FTIR, XPS, and PL spectra are presented. This material is available free of charge via the Internet at <http://pubs.acs.org>.

AUTHOR INFORMATION

Corresponding Authors

*E-mail: xiez@ciac.jl.cn (Z. X.).

*E-mail: sunzc@ciomp.ac.cn (Z. S.).

Author Contributions

The manuscript was written through contributions of all authors.

Notes

The authors declare no competing financial interest.

ACKNOWLEDGMENTS

The project was supported by Open Research Fund of State Key Laboratory of Polymer Physics and Chemistry. The financial support from the National Natural Science Foundation of China (No. 21201159, 61176016, and 21104075), China Postdoctoral Science Foundation Grant (No. 2012M510892), and the Ministry of Science is gratefully acknowledged. Z.S. thanks the support of the “Hundred Talent Program” of CAS and Innovation and Entrepreneurship Program of Jilin. Z.X. thanks the support of CIAC start-up fund.

REFERENCES

- (1) Baral, A.; Engelken, R. D. *Environ. Sci. Policy* **2002**, *5*, 121–133.
- (2) Zhitkovich, A. *Chem. Res. Toxicol.* **2011**, *24*, 1617–1629.
- (3) World Health Organization. *Guidelines for Drinking Water Quality*; World Health Organization: Geneva, Switzerland, 1997.

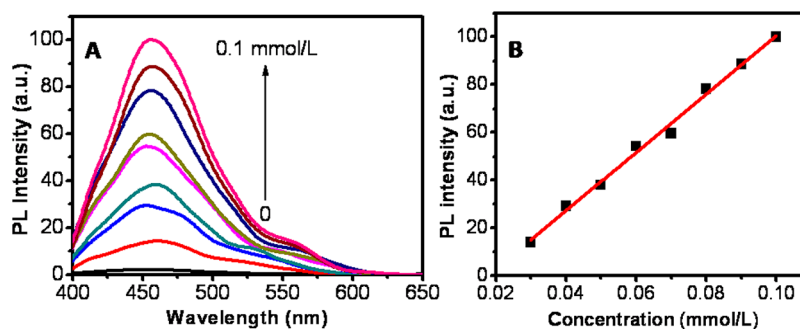


Figure 5. (A) Fluorescence response of the CD–Cr(VI) mixture to ascorbic acid at varied concentrations (0, 0.03, 0.04, 0.05, 0.06, 0.07, 0.08, 0.09, and 0.10 mmol/L). (B) The plot of the fluorescence intensity against the AA concentration in the range of 0.03–0.1 mmol/L.

- (4) Brauer, S. L.; Wetterhahn, K. E. *J. Am. Chem. Soc.* **1991**, *113*, 3001–3007.
- (5) Arancibia, V.; Valderrama, M.; Silva, K.; Tapia, T. *J. Chromatogr. B* **2003**, *785*, 303–309.
- (6) Xiang, Y.; Mei, L.; Li, N.; Tong, A. *J. Anal. Chim. Acta* **2007**, *581*, 132–136.
- (7) Anthemidis, A. N.; Zachariadis, G. A.; Kougoulis, J. S.; Stratis, J. *A. Talanta* **2002**, *57*, 15–22.
- (8) Hosseini, M.; Gupta, V. K.; Ganjali, M. R.; Rafiei-Sarmazdeh, Z.; Faridbod, F.; Goldooz, H.; Badiie, A. R.; Norouzi, P. *Anal. Chim. Acta* **2012**, *715*, 80–85.
- (9) Arrigoni, O.; Tullio, C. D. *Biochim. Biophys. Acta* **2002**, *11569*, 1–9.
- (10) Pisoschil, M.; Negulescu, G. P. *Biochem. Anal. Biochem.* **2011**, *1*, 106.
- (11) Baker, S. N.; Baker, G. A. *Angew. Chem., Int. Ed.* **2010**, *49*, 6726–6744.
- (12) Li, H. T.; He, X. D.; Liu, Y.; Huang, H.; Lian, S. Y.; Lee, S. T.; Kang, Z. H. *Carbon* **2011**, *49*, 605–609.
- (13) Li, H. T.; Kang, Z. H.; Liu, Y.; Lee, S. T. *J. Mater. Chem.* **2012**, *22*, 24230–24253.
- (14) Li, H. T.; He, X. D.; Kang, Z. H.; Huang, H.; Liu, Y.; Liu, J. L.; Lian, S. Y.; Tsang, C. C. A.; Yang, X. B.; Lee, S. T. *Angew. Chem., Int. Ed.* **2010**, *49*, 4430–4434.
- (15) Anilkumar, P.; Wang, X.; Cao, L.; Sahu, S.; Liu, J. H.; Wang, P.; Korch, K.; Tackett, K. N.; Parenzan, A.; Sun, Y. P. *Nanoscale* **2011**, *3*, 2023–2027.
- (16) Bhunia, S. K.; Saha, A.; Maity, A. R.; Ray, S. C.; Jana, N. R. *Sci. Rep.* **2013**, *3*, 1473.
- (17) Jia, X.; Li, J.; Wang, E. *Nanoscale* **2012**, *4*, 5572–5575.
- (18) Krysmann, M. J.; Kelarakis, A.; Dallas, P.; Giannelis, E. P. *J. Am. Chem. Soc.* **2012**, *134*, 747–750.
- (19) Kong, B.; Zhu, A. W.; Ding, C. Q.; Zhao, X. M.; Li, Bo.; Tian, Y. *Adv. Mater.* **2012**, *24*, 5844–5848.
- (20) Zhou, L.; Lin, Y. H.; Huang, Z. Z.; Ren, J. S.; Qu, X. G. *Chem. Commun.* **2012**, *48*, 1147–1149.
- (21) Li, H. L.; Zhai, J. F.; Sun, X. P. *Langmuir* **2011**, *27*, 4305–4308.
- (22) Li, H. L.; Zhai, J. F.; Tian, J. Q.; Luo, Y. L.; Sun, X. P. *Biosens. Bioelectron.* **2011**, *26*, 4656–4660.
- (23) Qu, Q.; Zhu, A.; Shao, X.; Shi, G.; Tian, Y. *Chem. Commun.* **2012**, *48*, 5473–5475.
- (24) Liu, J. M.; Lin, L.; Wang, X. X.; Lin, S. L.; Cai, W. L.; Zhang, L. H.; Zheng, Z. Y. *Analyst* **2012**, *137*, 2637–2642.
- (25) Liu, S.; Tian, J.; Wang, L.; Zhang, Y.; Qin, X.; Luo, Y.; Asiri, A. M.; Al-Youbi, A. O.; Sun, X. *Adv. Mater.* **2012**, *24*, 2037–2041.
- (26) Zhao, H. X.; Liu, L. Q.; Liu, Z. D.; Wang, Y.; Zhao, X. J.; Huang, C. Z. *Chem. Commun.* **2011**, *47*, 2604–2606.
- (27) Bai, W. J.; Zheng, H. Z.; Long, Y. J.; Mao, X. J.; Gao, M.; Zhang, L. Y. *Anal. Sci.* **2011**, *27*, 243–246.
- (28) Li, H. L.; Zhang, Y. W.; Wang, L.; Tian, J. Q.; Sun, X. P. *Chem. Commun.* **2011**, *47*, 961–963.
- (29) Shi, W. B.; Wang, Q. L.; Long, Y. J.; Cheng, Z. L.; Chen, S. H.; Zheng, H. Z.; Huang, Y. M. *Chem. Commun.* **2011**, *47*, 6695–6697.
- (30) Zhou, L.; Lin, Y. H.; Huang, Z. Z.; Ren, J. S.; Qu, X. G. *Chem. Commun.* **2012**, *48*, 1147–1149.
- (31) Wu, J.; Liu, W.; Ge, J.; Zhang, H.; Wang, P. *Chem. Soc. Rev.* **2011**, *40*, 3483–3495.
- (32) Zhang, D. W.; Dong, Z. Y.; Jiang, X. Z.; Feng, M. Y.; Li, W.; Gao, G. H. *Anal. Methods* **2013**, *5*, 1669–1675.
- (33) Shao, N.; Zhang, Y.; Cheung, S. M.; Yang, R. H.; Chan, W. H.; Mo, T.; Li, K. A.; Liu, F. *Anal. Chem.* **2005**, *77*, 7294–7303.
- (34) Yang, X. F.; Liu, P.; Wang, L. P.; Zhao, M. L. *J. Fluoresc.* **2008**, *18*, 453–459.
- (35) Shang, L.; Dong, S. J. *Anal. Chem.* **2009**, *81*, 1465–1470.
- (36) Shang, L.; Qin, C. J.; Jin, L. H.; Wang, L. X.; Dong, S. J. *Analyst* **2009**, *134*, 1477–1482.
- (37) Xu, L.; Li, B. X.; Jin, Y. *Talanta* **2011**, *84*, 558–564.
- (38) Tian, L.; Ghosh, D.; Chen, W.; Pradhan, S.; Chang, X.; Chen, S. *Chem. Mater.* **2009**, *21*, 2803–2809.
- (39) Kwon, W.; Rhee, S. W. *Chem. Commun.* **2012**, *48*, 5256–5258.
- (40) Qu, D.; Zheng, M.; Du, P.; Zhou, Y.; Zhang, L. G.; Li, D.; Tan, H. Q.; Zhao, Z.; Xie, Z. G.; Sun, Z. C. *Nanoscale* **2013**, DOI: 10.1039/C3NR04402E.
- (41) Dong, Y. Q.; Pang, H. C.; Yang, H. B.; Guo, C. X.; Shao, J. W.; Chi, Y. W.; Li, C. M.; Yu, T. *Angew. Chem., Int. Ed.* **2013**, *52*, 7800–7804.
- (42) Dong, Y. Q.; Shao, J. W.; Chen, C. Q.; Li, H.; Wang, R. X.; Yuwu Chi, Y. W.; Lin, X. M.; Chen, G. N. *Carbon* **2012**, *50*, 4738–4743.
- (43) Barrera-Díaz, C. E.; Lugo-Lugo, V.; Bilyeu, B. J. *Hazard. Mater.* **2012**, *223–224*, 1–12.
- (44) Xu, X. R.; Li, H. B.; Gu, J. D. *Environ. Toxicol. Chem.* **2005**, *24*, 1310–1314.
- (45) Dhala, B.; Thatoib, H. N.; Dasc, N. N.; Pandey, B. D. *J. Hazard. Mater.* **2013**, *250–251*, 272–291.